Disruption and Activation of Blood Platelets in Contact with an Antimicrobial Composite Coating Consisting of a Pyridinium Polymer and AgBr Nanoparticles

Kris N. Stevens,[†,‡] Menno L. Knetsch,[†] Ayusman Sen,[§] Varun Sambhy,[§] and Leo H. Koole*[,†]

CARIM Centre for Biomaterials Research, Faculty of Health, Medicine and Life Sciences, Maastricht University, Maastricht, The Netherlands, Department of Cardiothoracic Surgery, Maastricht University Medical Centre, Maastricht, The Netherlands, and Department of Chemistry, The Pennsylvania State University, University Park, Pennsylvania 16802

ABSTRACT Composite materials made up from a pyridinium polymer matrix and silver bromide nanoparticles embedded therein feature excellent antimicrobial properties. Most probably, the antimicrobial activity is related to the membrane-disrupting effect of both the polymer matrix and Ag^+ ions; both may work synergistically. One of the most important applications of antimicrobial materials would be their use as surface coatings for percutaneous (skin-penetrating) catheters, such as central venous catheters (CVCs). These are commonly used in critical care, and serious complications due to bacterial infection occur frequently. This study aimed at examining the possible effects of a highly antimicrobial pyridinium polymer/AgBr composite on the blood coagulation system, i.e., (i) on the coagulation cascade, leading to the formation of thrombin and a fibrin cross-linked network, and (ii) on blood platelets. Evidently, pyridinium/AgBr composites could not qualify as coatings for CVCs if they trigger blood coagulation. Using a highly antimicrobial composite of poly(4-vinylpyridine)-*co*-poly(4-vinyl-*N*-hexylpyridinium bromide) (NPVP) and AgBr nanoparticles as a thin adherent surface coating on Tygon elastomer tubes, it was found that contacting blood platelets rapidly acquire a highly activated state, after which they become substantially disrupted. This implies that NPVP/AgBr is by no means blood-compatible. This disqualifies the material for use as a CVC coating. This information, combined with earlier findings on the hemolytic effects (i.e., disruption of contacting red blood cells) of similar materials, implies that this class of antimicrobial materials affects not only bacteria but also mammalian cells. This would render them more useful outside the biomedical field.

KEYWORDS: catheter • silver • surface modification • thrombogenicity • nanoparticle • platelet activation

1. INTRODUCTION

Recently, it was discovered that composite materials consisting of a cationic pyridinium polymer matrix and AgBr nanoparticles embedded therein have pronounced antibacterial properties (1). This observation was primarily made with the copolymer poly(4-vinylpyridine)-*co*-poly(4-vinyl-*N*-hexylpyridinium bromide) (NPVP). Once placed on surfaces that were overgrown by bacteria (either gram-positive or gram-negative), the NPVP/AgBr composites killed all bacteria under and around them. Furthermore, the antibacterial effect lasted for relatively long periods, i.e., up to several days or weeks (1). Many parameters could be controlled (e.g., size of the AgBr nanoparticles, content of AgBr in the material, and release kinetics of Ag^+ ions). It was postulated that the mechanism of action is disruption of the bacterial membrane (initially), followed by sustained release of Ag^+ ions, even if the surface is covered with dead bacteria or biofilm (1).

There is a clear need for antimicrobial materials and coatings in many different fields of application. We are convinced that one of these applications would relate to percutaneous (skin-penetrating) catheters, especially so-called *central venous catheters* (CVCs). Such catheters are used extensively in the care of critical patients, for both monitoring and therapy. The use of CVCs is, however, associated with two significant problems: one is *bacterial colonization*, and the other is *blood coagulation* (2−4). The adherence of bacteria onto the surface of CVCs may lead to bloodstream infections, which are, in turn, associated with substantial morbidity, mortality, prolonged hospital stay, and increased cost. Recently, it was reported that the risk for bloodstream infection that is associated with the most common type of CVC (the noncuffed type) is as high as 2−7 episodes per 1000 catheter days (5). Coagulation, initiated by the part of the CVC that is in contact with the blood, can lead to the formation of thrombotic particulate emboli. When these detach from the CVC's surface, they can cause occlusion of relatively larger vital arteries in the lungs or in the brain (stroke), which may have detrimental consequences (4).

* Corresponding author. Tel: +31 43 3881531. Fax: +31 43 388 4159. E-mail: l.koole@bioch.unimaas.nl.
Received for review June 12, 2009 and accepted August 15, 2009
[†] Maastricht University.
[‡] Maastricht University Medical Centre.
[§] The Pennsylvania State University.
DOI: 10.1021/am900390h

Table 1. Overview of the Catheter Materials Used Throughout This Study

catheter	commercial source	coating	inner diameter (mm)	outer diameter (mm)
HemoGlide[a]	yes	no	2 lm; 2.3 mm each	4.8
PVC-Carmeda[b]	yes	antithrombotic Carmeda coating (heparin)	4.8	7.9
PVC[c]	yes	no	4.8	7.9
Tyg[d]	yes	no	4.8	6.4
Tyg-NPVP	no	cationic NPVP coating[e]	4.8	6.4
Tyg-NPVP/AgBr	no	cationic NPVP coating containing silver bromide (AgBr) nanoparticles[e]	4.8	6.4

[a] Purchased from Bard Nordic (Helsingborg, Sweden; ref 5664190). [b] Purchased from Medtronic Nederland (Heerlen, The Netherlands; ref M311902A). [c] Purchased from Medos Medizintechnik AG (Stolberg, Germany; ref 039682). [d] Purchased from Saint-Gobain Performance Plastics (Charny, France; ref Tygon S-50-HL AAX00011). [e] Prepared as a part of this study.

Clearly, NPVP/AgBr composites would not qualify as CVC coatings—despite their excellent antimicrobial properties—if the cationic polymer and/or the AgBr nanoparticles would result in a hemolytic and/or thrombogenic surface. With respect to hemolysis, it has been reported already that positively charged pyridinium polymers can lead to disruption of contacting red blood cells (hemolysis), especially when the positive charges at the material's surface are relatively far apart from each other (6). To the best of our knowledge, the aptitude of pyridinium polymers to initiate coagulation of the blood has not been studied. Therefore, we became interested in examining the blood compatibility of NPVP/AgBr composites. Here, we describe an in vitro study on a NPVP/AgBr composite in contact with fresh human platelet-rich blood plasma (PRP). Blood from six healthy volunteer donors was used. The NPVP/AgBr composite coating was applied onto tubes made out of Tygon, a biocompatible elastomer material that is applied in many different catheters. Unmodified Tygon tubes and Tygon tubes with a silver-free NPVP coating were used as controls. In some experiments, we also included commercially available CVC materials for reference. We studied surface-induced thrombin generation, activation of blood platelets due to contact with the surface coating, and morphology of adhered platelets. The results are discussed in the context of the potential utility of NPVP/AgBr composites as coatings for indwelling medical devices that are intended to function for extended periods (up to several weeks).

2. MATERIALS AND METHODS

2.1. Materials. Samples were prepared from Tygon tubing (Tyg). Tygon is a highly stable polymer material that is used in the catheter industry. NPVP and NPVP/AgBr were synthesized by the Pittsburgh group, according to protocols that were published previously (1). The materials were applied as adherent coatings onto the outer and inner surfaces of pieces of Tyg (Tyg-NPVP and Tyg-NPVP/AgBr; length of approximately 10 cm), by the same group. As controls, we used poly(vinyl chloride) (PVC) tubing of the same dimensions, PVC tubing carrying the Carmeda-immobilized heparin coating (also of the same dimensions; PVC-Carmeda), and/or the Bard HemoGlide CVC (HemoGlide) (7), which is the CVC that is used mostly in different Departments of the Maastricht University Medical Centre. Table 1 provides a comprehensive overview.

NaCl, $CaCl_2(H_2O)_2$, 25% glutaraldehyde, dimethyl sulfoxide, and Triton X-100 were purchased from Acros Organics (Geel, Belgium). Trisodium citrate and K_2HPO_4 were products from Sigma-Aldrich Chemie BV (Zwijndrecht, The Netherlands). KH_2PO_4 was from Janssen Chimica (Beerse, Belgium), and 100% ethanol was from Merck KGaA (Darmstadt, Germany). Lepirudin (Refludan) was obtained from Pharmion (Windsor Berkshire, U.K.). The fluorogenic substrate for thrombin, Z-Gly-Gly-Arg-AMC, was a product of Bachem Holding AG (Bubendorf, Switzerland; ref I-1140). The platelet-stabilizing anticoagulant mixture, citrate-theophylline-adenosine-dipyridamole (CTAD), was purchased from Becton Dickinson (Alphen aan den Rijn, The Netherlands). The lactate dehydrogenase (LDH) assay was performed using the CytoTox 96 Non-Radioactive Cytotoxicity Assay from Promega Benelux BV (Leiden, The Netherlands). Platelet activation was quantified with the Asserachrom β-TG enzyme-linked immunosorbent assay (ELISA), obtained from Roche Diagnostics Nederland BV (Almere, The Netherlands).

2.2. Equipment. Platelets were counted on an automatic cell counter (Coulter AC-T diff, Beckman Coulter, Miami, FL). Fluorescence tracings were recorded on a SpectraMax M2 spectrofluorometer (Molecular Devices, Sunnyvale, CA). Absorbances were measured on an ELx808 Absorbance Microplate Reader (BioTek Instruments, Inc., Winooski, VT). Sputter coating was performed with a 108 auto/SE sputter coater (Cressington Scientific Instruments Ltd., Watford, U.K.), and for scanning electron microscopy (SEM) analysis, a Philips XL30 scanning electron microscope (Philips, Eindhoven, The Netherlands) was used. Centrifugation was performed in a MSE Mistral 3000 I centrifuge (Beun-de Ronde, Abcoude, The Netherlands).

2.3. Preparation of the Catheter Samples. Catheter samples were cut to the correct dimensions (vide infra) in a laminar flow cabinet. The catheter Tyg was used as a reference in all of our experiments. In most of our experiments, we used the catheter samples directly as incubation wells by closing one end with a surgical tube clamp (8).

We also tested commercially available control materials in parallel throughout our experiments. However, the dimensions of these commercial products did not allow them to be used consistently throughout all experiments.

The HemoGlide catheter is the CVC of choice in our institution. It was used in all of our thrombin generation assays. However, because of its double lumen, it was impossible to use HemoGlide in the other assays.

PVC tubing (single lumen), with and without the Carmeda coating, was used as a reference material in our LDH assays, in our SEM analyses, and in our platelet activation assay. However, the thickness of the wall precluded the use of these materials in our thrombin generation assay.

2.4. Blood Collection and Preparation of PRP. Blood was collected through venipuncture from 6 healthy nonsmoking male volunteer donors, who did not take any hemostasis-

influencing medication at least 10 days before the experiment. Depending on the experiment to be performed, the blood was anticoagulated immediately with either citrate (end concentration: 0.013 M citrate) or lepirudin, a recombinant form of hirudin (end concentration: 20 μg/mL lepirudin). Lepirudin is a direct thrombin inhibitor and executes its anticoagulant effect without interfering with platelet function (9−11). Therefore it is the anticoagulant of choice for platelet activation studies. Then, PRP was isolated from the blood through centrifugation (200*g*, 15 min, room temperature) (8, 12, 13). Before the start of each experiment, the concentration of platelets in the PRP was measured with an automatic cell counter.

2.5. Platelet Adhesion Assay. The CytoTox 96 Non-Radioactive Cytotoxicity Assay measures the number of viable platelets adhered to a specific surface area of a biomaterial via colorimetric quantification of the enzyme LDH, released upon cell lysis. The experiment was performed twice with PRP from two different donors {donor 2 ([platelets] = 418 × 10^3 μL^{-1}) and donor 4 ([platelets] = 446 × 10^3 μL^{-1})}. Throughout each experiment, all catheter groups were tested in triplicate with identical PRP.

At the start of each experiment, 200 μL of citrated PRP was added to each clamped catheter tube, followed by 1 h of incubation at 37 °C. The samples were rinsed three times with 200 μL of phosphate-buffered saline (PBS; 10 mM K_2HPO_4, 10 mM KH_2PO_4, 150 mM NaCl; pH 7) to remove loosely adhered platelets. The remaining bound platelets were lysed to release LDH by adding 200 μL of a lysis solution (0.8% Triton X-100) and incubating 1 h at room temperature. From each catheter sample, 50 μL of a lysis solution was transferred in triplicate to the wells of a 96-well plate. Next, 50 μL of a substrate mix, containing a tetrazolium salt, was added to each well, directly followed by incubation in the dark for 30 min at room temperature. The tetrazolium salt is converted by LDH into a red formazan product. Finally, 50 μL of a stop solution was added to each well, and the optical density was measured at 490 nm. Viable platelets, adhered to each catheter tube, were quantified by a standard curve plotted from samples containing known amounts of platelets.

2.6. Morphology of Adhered Platelets. These experiments were performed with PRP from donor 4 ([platelets] = 453 × 10^3 μL^{-1}) in parallel with the platelet adhesion assay (see above). Citrated PRP (200 μL) was added to each clamped catheter tube followed by 1 h of incubation at 37 °C. Loosely adhered platelets were removed by rinsing the catheter tubes three times with 200 μL of PBS. The remaining bound platelets were fixed onto the catheter surfaces by incubating the samples for 10 min in 2.5% glutaraldehyde at 4 °C. Samples were dehydrated by 10 min of incubation at room temperature in increasing ethanol concentrations of 50, 70, 80, 95, and 100%. Then, the samples were freeze-dried. From each sample, three cylindrical pieces were cut with a length of 5 mm. Each of these cylindrical pieces was then cut longitudinally into four equal-sized pieces. This resulted for each catheter group in a total number of 12 catheter pieces for evaluation. Each catheter piece was glued onto a stub, sputter-coated with gold, and finally analyzed using SEM. Images were captured at 10 kV, with magnifications of 1080× and 4320×. For each catheter piece, two SEM images were captured at each magnification, resulting in 24 SEM images per magnification per catheter group. Platelet adhesion was quantified by counting platelets on 4320×-magnified SEM images. The platelet morphology was analyzed using Goodman's classification describing platelet morphologies on biomaterial surfaces (14). Catheter groups were tested in triplicate.

2.7. Platelet Activation. These experiments were performed with PRP from donor 4 ([platelets] = 402 × 10^3 μL^{-1}) in parallel with the platelet adhesion and platelet morphology assays (see above). Lepirudin-anticoagulated PRP (250 μL) was added to each clamped catheter tube and incubated for 1 h at 37 °C. Following incubation, 250 μL of PRP was sampled from each catheter tube and directly anticoagulated with 30 μL of CTAD. Identically, a 250 μL PRP sample was taken at the start of the experiment, to determine baseline platelet activation, which could have occurred during isolation of PRP. Further processing of the PRP samples and quantification of platelet activation were performed using the Asserachrom β-TG ELISA according to the instructions of the manufacturer. Every catheter group was tested in triplicate.

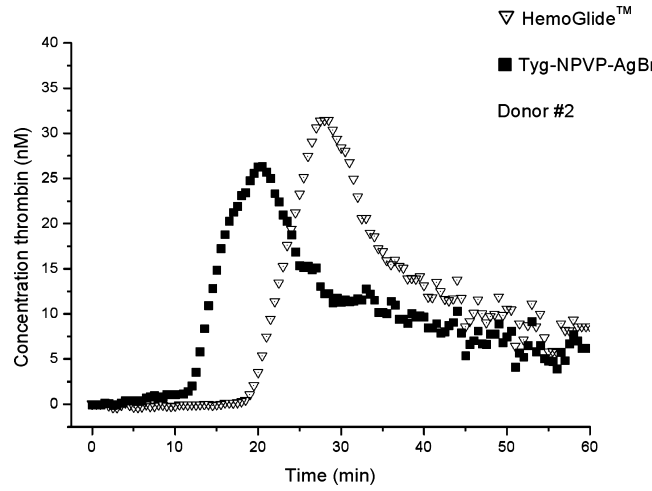

FIGURE 1. Thrombin generation curves measured with a HemoGlide Tyg-NPVP/AgBr sample. Both experiments were performed simultaneously with PRP from a single donor (donor 2). Notice how the time span between the onset of the experiment and the sudden rise in thrombin levels differs.

2.8. Thrombin Generation. Each thrombin generation experiment was performed with PRP from a single donor. This allowed all catheter groups to be tested with identical PRP. The experiment was performed six times with PRP from six different donors. In each experiment, every catheter group was tested in 6-fold.

Catheter samples (length: 4 mm) were placed horizontally in the wells of a 96-well plate (8). Just before the start of the experiment, a fluorogenic substrate for thrombin, Z-Gly-Gly-Arg-AMC, was added to citrated PRP to a final concentration of 400 μM. Next, the citrated PRP was "recalcified" by adding a $CaCl_2$ stock solution (0.5 M $CaCl_2$) to a final concentration of 20 mM $CaCl_2$. Upon recalcification, concentrations of Ca^{2+} were restored to physiological levels, and the blood clot mechanism is no longer inhibited.

Then, PRP + fluorogenic substrate was instantly distributed over the wells in volumes of 200 μL. Wells without a catheter sample served as controls.

Fluorescence tracings were recorded at 37 °C, every 30 s for 1 h (λ_{ex} = 368 nm and λ_{em} = 460 nm and 2 s of shaking prior to each measurement) (15). The fluorescence intensity was converted into nanomolar concentrations of thrombin, as described earlier by Hemker et al. (16). This resulted in a thrombin generation curve for each well, as shown in Figure 1.

The thrombin generation assay can best be explained by comparing the control material, HemoGlide, and the Tyg-NPVP/AgBr catheter. The control experiment [PRP/substrate/Ca^{2+} mixture incubated in the presence of the HemoGlide catheter (Δ)] shows a typical control thrombin generation curve, which depicts the change of [thrombin] versus time. During the first minutes, [thrombin] remains close to zero. Then, a sudden increase of [thrombin] is seen. The concentration rises steeply, passes a maximum, and slowly decreases to (approximately) zero. The formation of thrombin is the result of intrinsic coagulation (contact with foreign materials).

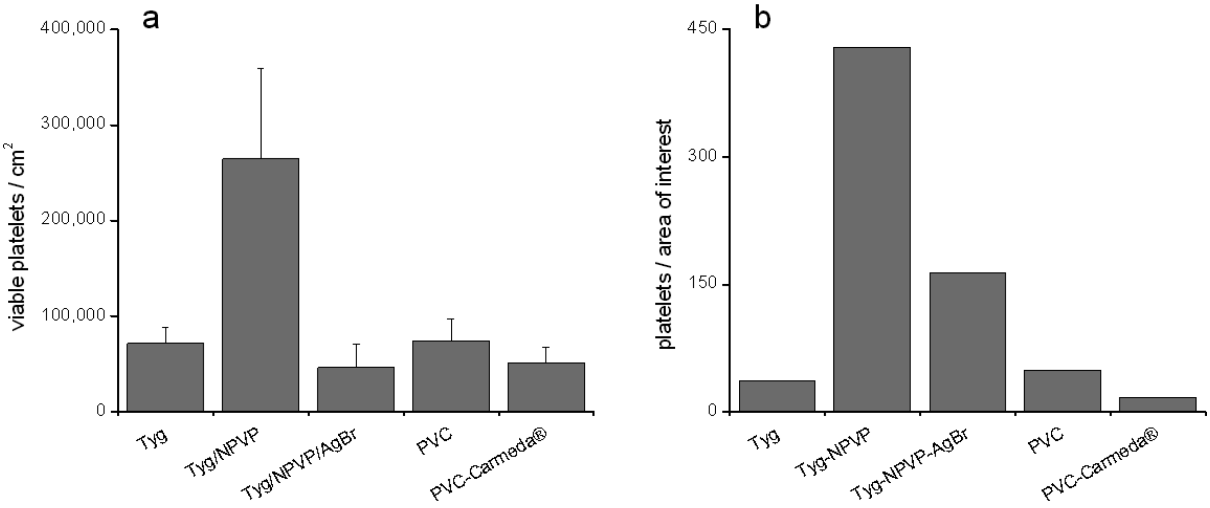

FIGURE 2. Platelet adhesion onto Tyg, Tyg-NPVP, Tyg-NPVP/AgBr, PVC, and PVC-Carmeda catheters. The graph combines the results from both the LDH assay (a) and SEM analysis (b). During both experiments, catheter groups were tested in triplicate. Data are shown as the mean ± standard deviation in panel a and, in panel b, as the number of platelets counted on all SEM images for each specific catheter group.

In the presence of a Tyg-NPVP/AgBr catheter in the well (!), the thrombin generation curve changes, especially in the sense that the time interval between the start of the experiment and the sudden rise of [thrombin] becomes shorter. This time interval, also called the thrombin generation lag time (TGT_{lag}), was measured systematically in this study and was defined as the time span between the onset of the experiment and the time point at which an increase of ≥2 nM thrombin is attained between two time points. Materials with lesser hemocompatibility typically display shorter thrombin generation lag times.

3. RESULTS

3.1. Platelet Adhesion Assay. These experiments were performed with PRP from two different donors (donors 2 and 4); Figure 2a compiles the results for donor 4. Results were very similar for donor 2 (data not shown). Clearly, the Tyg-NPVP material has the highest density of adhered viable platelets at the surface (approximately 270 000 cm^{-2}). Surprisingly, the incorporation of AgBr nanoparticles in the coating strongly reduces the adsorption of viable platelets to approximately 50 000 cm^{-2}. Similar densities of adhered platelets were found for the other three (control) materials. Figure 2b displays the number of platelets counted via SEM, irrespective of their morphology (or viability).

3.2. Morphology of Adhered Platelets. These experiments were done in parallel with the LDH assay (see above), using PRP from donor 4 and the same biomaterials. SEM is known to be an excellent technique to study the morphology of blood platelets after their adherence to biomaterial surfaces (17). Figure 3 shows representative SEM micrographs of platelets adhered to the different catheter tubes. In line with the data from the LDH assay, most platelets were found on the Tyg-NPVP surface. To a large extent, the morphologies of these platelets were spread and dendritic with relatively long pseudopodia. An increased surface density of adhered platelets was also seen on the surface of Tyg-NPVP/AgBr samples, compared to Tyg, PVC, and PVC-Carmeda control samples. This differs from the data obtained with the LDH assay (Figure 2a). Additionally, morphologies were remarkably different: most of the platelets adhered to Tyg-NPVP/AgBr appeared dendritic with numerous short pseudopodia; i.e., they were significantly distorted. Apparently, the presence of AgBr nanoparticles in the coating strongly affects the morphology and viability of contacting blood platelets.

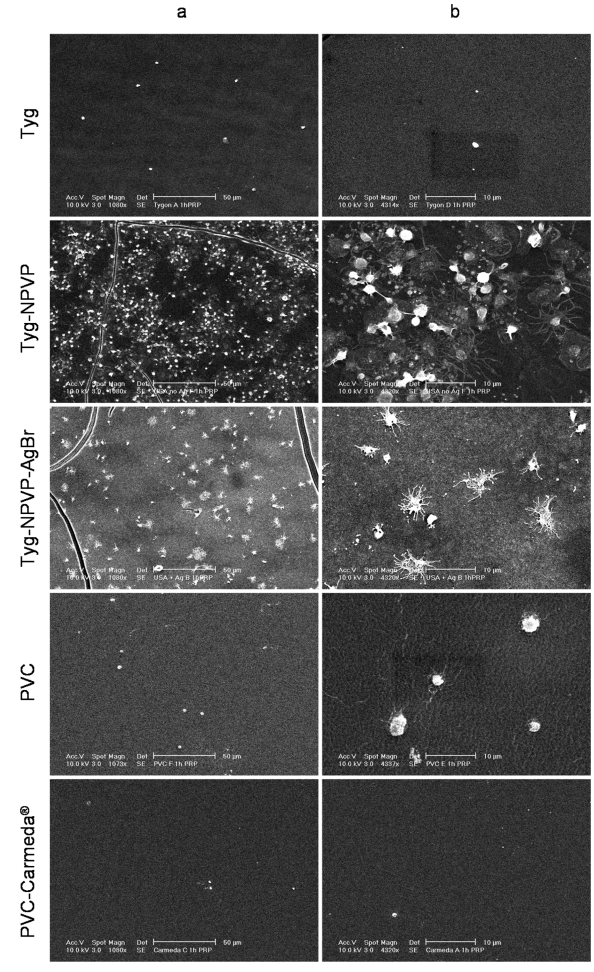

FIGURE 3. Results of SEM analyses for Tyg, Tyg-NPVP, Tyg-NPVP/AgBr, PVC, and PVC-Carmeda catheters. For each catheter group, two representative SEM images, with magnifications of 1080× (a) and 4320× (b), are shown.

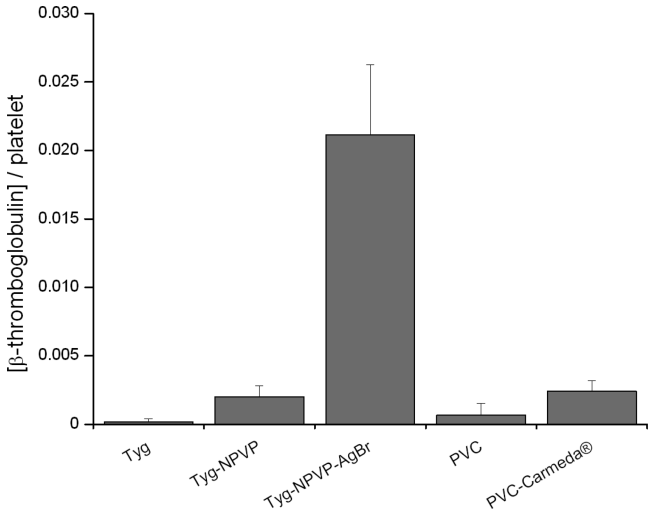

FIGURE 4. Analysis of platelet activation. Levels of β-thromboglobulin were elevated in Tyg-NPVP/AgBr catheters. Experiments were performed in triplicate. Data from the platelet activation assay were corrected for baseline platelet activation. For each catheter group, concentrations of β-thromboglobulin (IU/mL) were divided by the mean density of platelets (cm^{-2}) present on the respective catheter surfaces. Data are presented as the mean $\pm$ standard deviation.

3.3. Platelet Activation. These experiments were done in parallel with the LDH assay and the SEM experiments described above, using PRP from donor 4 and the same biomaterials. The results are normalized for the number of adhered viable platelets and are shown in Figure 4. Platelets in contact with Tyg, Tyg-NPVP, PVC, or PVC-Carmeda coating do not become activated to a measurable extent: the β-thromboglobulin levels remain rather low.

On the other hand, the Tyg-NPVP/AgBr surface induced marked activation, as is evidenced by an approximately 10-fold higher amount of β-thromboglobulin released per platelet. Remarkably, the relatively high levels of β-thromboglobulin in the plasma coincide with a distorted morphology of platelets adhered at the surface. This is plausible because platelet lysis will result in leakage of the cellular contents, including β-thromboglobulin, into the surrounding medium.

3.4. Thrombin Generation. These experiments were done with fresh PRP from six healthy male donors and four different biomaterials: Tyg-NPVP/AgBr-coated tubes, Tyg-NPVP-coated tubes, Tyg tubes, and the HemoGlide catheter. Measurement of the thrombin generation curve is one of the best methods to assessthe thrombogenicity of artificial materials (18, 19). Here, we chose to use the static assay and PRP (8, 12). In principle, thrombin generation can also be measured in a flow system, using whole blood. However, because of the relatively large bore of our samples, the dynamic assay would have required more than 1 L of fresh human blood per sample, which was clearly impossible.

As is well-known, the contact of blood with a foreign surface triggers the intrinsic pathway (19). The intrinsic and extrinsic pathways coincide at the level of factor Xa. Then, downward in the coagulation cascade, the result is the formation of thrombin, which will ultimately catalyze the conversion of fibrinogen into fibrin.

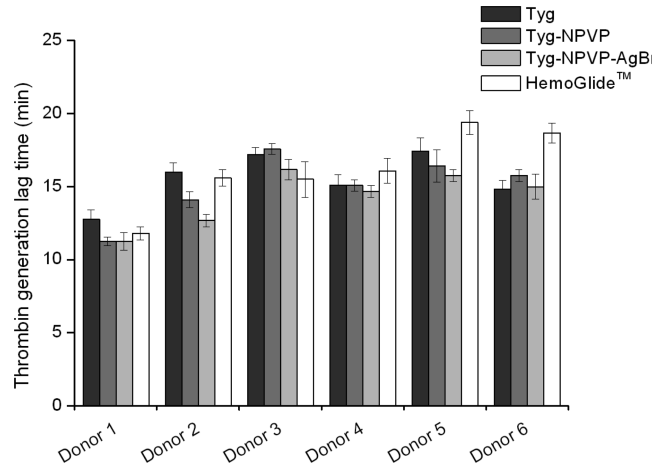

FIGURE 5. Thrombin generation assays for six different donors. Thrombin generation lag times (TGT_{lag}) are presented for Tyg, Tyg-NPVP, Tyg-NPVP/AgBr, and HemoGlide catheters. Data are shown as the mean $\pm$ standard deviation. Experiments were performed in 6-fold.

The results of our thrombin generation measurements are shown in Figure 5. Note that these graphs plot the thrombin generation lag times (TGT_{lag}, vide supra) as measured at least in 4-fold per donor and per material.

The data in Figure 5 reveal that the TGT_{lag} values show a considerable donor dependency. For example, when the data that were obtained with the Tyg material (a control) are are compared, it is seen that the TGT_{lag} values rank as follows: donor 1 (13 ± 1 min) < donor 4 (15 ± 2 min) = donor 6 (15 ± 2 min) < donor 2 (16 ± 2 min) < donor 3 (17 ± 2 min) = donor 5 (17 ± 2 min). In other words, the fastest clotting was observed with the PRP from donor 1, while the slowest clotting was observed with the PRP from donors 3 and 5. Donor variations of approximately the same magnitude have been observed previously (8).

There is no consistent effect of the NPVP coating on the thrombin generation lag time. For donors 1, 2, and 5, a slight decrease of TGT_{lag} is observed, whereas no effect was found for donors 3 and 4. For donor 6, TGT_{lag} was found to increase slightly upon application of the NPVP coating.

Incorporation of the AgBr nanoparticles in the NPVP coating has a small accelerating effect on thrombin formation, at least for donors 2, 3, 5, and 6. With the PRP of donors 1 and 4, we found no effect of the TGT_{lag} values because of the presence of the AgBr nanoparticles.

Finally, the TGT_{lag} values measured with the HemoGlide catheter material are only slightly longer than those measured for Tyg-NPVP/AgBr. Considerable differences were found for donors 2, 5, and 6.

4. DISCUSSION

Our evaluation of the events that occur after contacting fresh human PRP (which contains the major players in hemostasis, i.e. the proteins that constitute the coagulation cascade, and the blood platelets) with the materials Tyg, Tyg-NPVP, Tyg-NPVP/AgBr, and control materials has led to several new insights. Perhaps the most important observation was that the Tyg-NPVP/AgBr surface induces *activation*

and *disruption* of the platelets. This was most evident from our measurements of β-thromboglobulin, a protein that is released by activated platelets (20). Examination of the surface of Tyg-NPVP/AgBr with SEM (after an incubation time of 1 h) showed extensively distorted morphologies of the adhered platelets. It is likely that this shape coincides with a high degree of activation and disruption. The previous work of Sambhy et al. (1) describes the elution of Ag^+ ions from the NPVP/AgBr coating. Whether elution of Ag^+ ions, and, subsequently, platelet activation in the suspension, can explain the observed platelet-activating effects is an interesting point. This possibility can be ruled out on the basis of three combined arguments: (i) Ag^+ ions have antimicrobial action if the concentration exceeds 100 nM (8); (ii) Ag^+ ions lead to platelet activation if their concentration exceeds 100 μM (8); (iii) the Ag^+ concentration as a result of leaching out of NPVP/AgBr coatings is approximately 4 ppm (1). The concentration of 4 ppm corresponds with 0.3 μM. This implies that media around these coatings are antimicrobial but do not induce platelet activation. Hence, we adhere to the explanation that the NPVP/AgBr surfaces have platelet-activating and disrupting features, not the media surrounding these surfaces.

Furthermore, we found that the thrombin generation assay could not discriminate between the "platelet-friendly" surfaces, on the one hand (i.e., Tyg, Tyg-NPVP, and the other controls), and the platelet-disrupting surface Tyg-NPVP/AgBr, on the other hand. This may indicate that the NPVP/AgBr-induced activation also precludes the phospholipid transition in the platelet membrane; this transition (also known as the flip-flop mechanism) is known to be mandatory in order to turn the platelet's membrane into a procoagulant surface (21, 22). The results from this study reveal that measurement of the thrombin generation curves alone is not sufficient to assess the blood compatibility of the artificial surfaces. It is absolutely necessary to examine the platelets (and especially their status in terms of activation) as well.

5. CONCLUSIONS

The pronounced antimicrobial activity of NPVP/AgBr composites makes these materials attractive candidates as coatings for catheters. The observed activating and disrupting effect on blood platelets disqualifies these materials as coatings for CVCs. Probably, pyridinium polymer/AgBr composites may prove to be extremely useful as antibacterial surfaces in applications outside the biomedical field, in which contact with cells other than bacteria is essentially irrelevant.

Acknowledgment. The authors thank Stefan G. J. A. Camps for his assistance during the laboratory experiments. This study was financed through the Bioterials program, a private-public joint effort of the Dutch Ministry of Economic Affairs, the Province of Dutch Limburg, DSM Research BV (Geleen, the Netherlands), and the Maastricht University Medical Center. This study was also supported by the Deutsche Forschungsgemeinschaft, through the Graduiertenkolleg "Biointerface-Detektion und Steuerung grenzflacheninduzierter, biomolekularer und zellularer Funktionen" (GRK 1035/2). The Universities of Aachen, Liege and Maastricht cooperate within the framework of this Graduiertenkolleg.

REFERENCES AND NOTES

(1) Sambhy, V.; MacBride, M. M.; Peterson, B. R.; Sen, A. *J. Am. Chem. Soc.* **2006**, *128*, 9798–9808.
(2) Ruschulte, H.; Franke, M.; Gastmeier, P.; Zenz, S.; Mahr, K. H.; Buchholz, S.; Hertenstein, B.; Hecker, H.; Piepenbrock, S. *Ann. Hematol.* **2009**, *88*, 267–272.
(3) Acedo Sánchez, J. D.; Batlle, J. F.; Feijoo, J. B. *Support Cancer Ther.* **2007**, *4*, 145–151.
(4) Burns, K. E.; McLaren, A. *Can. J. Anaest.* **2008**, *55*, 532–541.
(5) Zingg, W.; Cartier-Faessler, V.; Walder, B. *Best Pract. Res. Clin. Anaest.* **2008**, *22*, 407–420.
(6) Sambhy, V.; Peterson, B. R.; Sen, A. *Angew. Chem., Int. Ed.* **2008**, *47*, 1250–1254.
(7) See: www.bardaccess.com.
(8) Stevens, K. N.; Crespo-Biel, O.; van den Bosch, E. E.; Dias, A. A.; Knetsch, M. L. W.; Aldenhoff, Y. B.; van der Veen, F. H.; Maessen, J. G.; Stobberingh, E. E.; Koole, L. H. *Biomaterials* **2009**, *30*, 3682–3690.
(9) Kopp, R.; Bernsberg, R.; Kashefi, A.; Mottaghy, K.; Rossaint, R.; Kuhlen, R. *Int. J. Artif. Organs* **2005**, *28*, 1272–1277.
(10) Kalb, M. L.; Potura, L.; Scharbert, G.; Kozek-Langenecker, S. A. *Platelets* **2009**, *20*, 7–11.
(11) Alban, S. *Curr. Pharm. Des.* **2008**, *14*, 1152–1175.
(12) Aldenhoff, Y. B. J.; Hanssen, J. H.; Knetsch, M. L.; Koole, L. H. *J. Vasc. Interv. Radiol.* **2007**, *18*, 419–425.
(13) Stevens, K. N.; Aldenhoff, Y. B. J.; van der Veen, F. H.; Maessen, J. G.; Koole, L. H. *J. Biomed. Biotechnol.* **2007**, *10*, 29464.
(14) Goodman, S. L. *J. Biomed. Mater. Res.* **1999**, *45*, 240–250.
(15) Wielders, S. J.; Ungethüm, L.; Reutelingsperger, C. P.; Bevers, E. M.; Lindhout, T. *Thromb. Haemost.* **2007**, *98*, 1056–1062.
(16) Hemker, H. C.; Giesen, P.; AlDieri, R.; Regnault, V.; de Smed, E.; Wagenvoord, R.; Lecompte, T.; Béguin, S. *Pathophysiol. Haemost. Thromb.* **2002**, *32*, 249–253.
(17) Rodrigues, S. N.; Goncalves, I. C.; Martins, M. C.; Barbosa, M. A.; Ratner, B. D. *Biomaterials* **2006**, *27*, 5357–5367.
(18) Saralidze, K.; van Hooy-Corstjens, C. S. J.; Koole, L. H.; Knetsch, M. L. W. *Biomaterials* **2007**, *28*, 2457–2464.
(19) Thor, A.; Rasmusson, L.; Wennerberg, A.; Thomsen, P.; Hirsch, J. M.; Nilsson, B.; Hong, J. *Biomaterials* **2007**, *28*, 966–974.
(20) Ohkawa, R.; Hirowatari, Y.; Nakamura, K.; Ohkubo, S.; Ikeda, H.; Okada, M.; Tozuka, M.; Nakahara, K.; Yatomi, Y. *Clin. Biochem.* **2005**, *38*, 1023–1026.
(21) Zwaal, R. F.; Confurius, P.; Bevers, E. M. *Cell. Mol. Life Sci.* **2005**, *62*, 971–988.
(22) Schoenwaelder, S. M.; Yuan, Y.; Josefsson, E. C.; White, M. J.; Yao, Y.; Mason, K. D.; O'Reilly, L. A.; Henley, K. J.; Ono, A.; Hsiao, S.; Wilcox, A.; Roberts, A. W.; Huang, D. C.; Salem, H. H.; Kile, B. T.; Jackson, S. P. *Blood* **2009**, *114*, 663–666.

AM900390H